Raman spectroscopy and scanning electron microscopy investigation of annealed amorphous carbon–germanium films deposited by d.c. magnetron sputtering

G. Mariotto [a], C. Vinegoni [a], L.G. Jacobsohn [b], F.L. Freire Jr. [b,*]

[a] *Istituto Nazionale per la Fisica della Materia and Dipartimento di Fisica, Università di Trento, 38050 Povo, TN, Italy*
[b] *Departamento de Física, Pontifícia Universidade Católica do Rio de Janeiro, Caixa Postal 38071, 22452-970 Rio de Janeiro, RJ, Brazil*

Abstract

The precipitation of germanium nanocrystals in amorphous carbon–germanium films allows for the development of innovative devices, but the accurate control of both size and size distribution of Ge quantum dots in these matrices still constitutes a challenging step. In this paper, both the structure and morphology of amorphous carbon–germanium films (a-$Ge_{1-x}C_x$), deposited by d.c. magnetron sputtering onto silicon substrates and annealed in vacuum at temperatures up to 550 °C, are investigated by Raman spectroscopy and scanning electron microscopy. The main features of Raman spectra obtained from carbon-rich films ($x > 0.43$) are the D and G bands, characteristic of graphitic carbon films. The ratio between the intensities of the bands, I_D/I_G, increases with the annealing temperature, suggesting a progressive increase of the graphitic domains within the films. Raman spectra obtained in the low frequency region from both as-deposited and annealed germanium-rich films ($x < 0.43$) show broad bands associated with transverse acoustic and transverse optic Ge–Ge modes. Ge–Ge optic modes merge up into a well-shaped peak at 300 cm^{-1} in the germanium-richest sample, and underwent annealing treatment at 550 °C, thus indicating the precipitation of crystalline Ge. Scanning electron microscopy analysis shows an apparently uniform nucleation of Ge crystallites at the sample surface. Microprobe Raman scattering results suggest the formation of a nearly homogeneous distribution of Ge nanocrystals in germanium-rich films annealed at 550 °C. © 1999 Elsevier Science S.A. All rights reserved.

Keywords: Amorphous carbon films; d.c. Magnetron sputtering; Nanocrystalline germanium; Raman spectroscopy

1. Introduction

In the last few years, the study of Ge quantum dots and of both $S_{1-x-y}Ge_xC_y$ and $Ge_{1-x}C_x$ heterostructures grown on Si has received increasing attention. Their optoelectronic properties and compatibility with existing silicon very-large-scale integration technology make them candidates for several innovative devices, i.e. light emitting diodes and quantum dot transistors [1–5]. The incorporation of substitutional carbon into Si–Ge alloys is very promising since, with a suitable amount of carbon, a 9:1 ratio of Ge:C assuming Vegard's law, the $S_{1-x-y}Ge_xC_y$ lattice parameter can be adjusted to that of Si. Thus, the carbon incorporation helps to circumvent one of the limitations for the development of SiGe technology, namely the critical thickness of epitaxial

film [6]. Besides, the Ge–C system itself is an alternative pathway for Si-based bandgap engineering [7].

As for Ge quantum dots, a very crucial step in view of technological applications is the ability to obtain uniformity in size and spatial distribution of the quantum dots [4]. With this aim, the use of an amorphous carbon matrix (a-C) for the confinement of Ge nanocrystals is expected to provide some advantages when compared with Ge$^+$-implanted SiO_2 or Ge–SiO_2 multilayer structures [8,9] due to the low C solubility in Ge (10^8 atoms/cm^3 at the melting point of Ge). In fact, the formation of crystalline Ge in a-$Ge_{1-x}C_x$ films was reported for samples prepared by metalorganic chemical vapor deposition at temperatures higher than 500 °C [10]. Recently, the use of a-Ge/a-C multilayers was proposed as an alternative suitable route for the control of Ge nanocrystals growth [11]. On the other hand, the optoelectronic properties of hydrogenated amorphous carbon–germanium films (a-$Ge_{1-x}C_x$:H)

---

* Corresponding author. Tel: +55 21 529 9360; fax: +55 21 259 9397;
e-mail: lazaro@fis.puc-rio.br

have been studied due to their potential use in thin film solar cells [12]. For all applications described above, the thermal stability of these films is an important parameter, since it will define the temperature range for operation of the devices or the compatibility with other technological processing steps.

In this work, we report on the results of Raman and scanning electron microscopy (SEM) investigations carried out on annealed a-Ge$_{1-x}$C$_x$ films deposited at room temperature onto $\langle 100 \rangle$ c-Si substrates by d.c. magnetron sputtering.

2. Experimental procedures

To incorporate Ge into amorphous carbon films deposited by d.c. magnetron sputtering, small strips of ultra-pure germanium were put on the surface of a graphite target (99.95% pure). A d.c. (-510 V) argon plasma operated at 0.36 Pa was used to sputter the target, while the sample holder was grounded and kept at room temperature. The thickness of the different films ranged from 200 nm to 1.4 μm, as measured by a stylus profilometer. Rutherford backscattering spectrometry (RBS) and elastic recoil detection analysis (ERDA) determined the chemical composition of the films. The film thickness combined with the areal density, given by ion beam analyses, provided the density of the films. The samples were annealed in vacuum for 1 h at fixed temperatures up to 550 °C, without any kind of sequential annealing on each sample. Further details on the film deposition procedure and chemical characterization were published elsewhere [13].

Raman scattering measurements were carried out at room temperature in a nearly backscattering geometry with the sample held in vacuum. A laser beam of low power density ($\lambda = 488.0$ nm, $P = 100$ mW, beam spot ~ 400 μm^2) was used to avoid any sample damage. Micro-Raman analyses were carried out in air. Both excitation ($\lambda = 488.0$ nm) and light collection occurred through an optical microscope (Olympus model BHSM-L-2) with a $100 \times$ objective, in backscattering geometry. The radiation was analyzed by a double monochromator (Jobin-Yvon, Ramanor model HGS-2), equipped with holographic gratings (2000 lines/mm) and was detected by a cooled GaAs photomultiplier operated in photon counting mode. The laser power was kept below 2 mW and the beam spot at the sample surface was of the order of 5 μm^2. The temperature of the samples during the measurements, both in macro and micro configurations, was estimated from the intensity ratio between Stokes and anti-Stokes scattering counterparts of the Raman spectrum via the Bose–Einstein factor for first-order events. In our experimental conditions, the temperature increase caused by the laser irradiation was of the order of a few tens of degrees Celsius, even in micro-

Table 1
Germanium/carbon atomic ratio, as measured by RBS, thickness and density of as-deposited a-Ge$_{1-x}$C$_x$ films

Sample	Ge/C ratio	Thickness (nm)	Density (10^{23} atoms/cm^3)
a-C	0	186	1.8
a-Ge$_{0.04}$C$_{0.96}$	0.035	228	1.4
a-Ge$_{0.57}$C$_{0.43}$	1.3	1330	0.7
a-Ge$_{0.76}$C$_{0.24}$	3.3	1445	0.5

Raman configuration. A Carl-Zeiss DSM 960 scanning electron was used for surface topography characterization.

3. Results and discussion

The ratio between the germanium and carbon concentrations, the film thickness and density for the samples studied in this work are listed in Table 1. Oxygen and hydrogen contamination (both typically of 4 at%) were determined by RBS and ERDA analyses, respectively. The ion beam techniques indicate that the film composition is essentially constant in the temperature range studied here, and only a loss of about 50% hydrogen was observed for samples annealed at 550 °C. Moreover, the film thickness and density did not change with thermal treatment.

Experimental Raman spectra of a-Ge$_{0.04}$C$_{0.96}$ films annealed at several temperatures are reported in Fig. 1. The spectra look very similar to those obtained from pure a-C films annealed under the same conditions. The only features observed in these spectra are the D and G bands characteristic of sp^2-bonded amorphous carbon
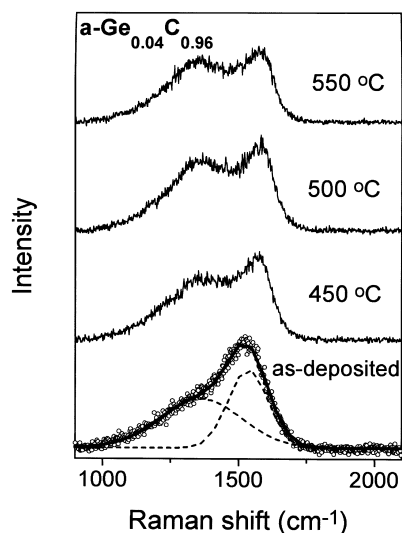

Fig. 1. Raman spectra obtained from a-Ge$_{0.04}$C$_{0.96}$ films annealed at several temperatures. The solid line is the fitted spectrum, as discussed in the text. The D and G bands are also plotted (dashed lines).

[14]. The G band, peaked at about $1540 \, cm^{-1}$, is associated with the allowed E_{2g} optical modes of the Brillouin zone center of the crystalline graphite, while the D band, occurring at approximately $1360 \, cm^{-1}$, is attributed to disorder-allowed phonon modes, which become Raman active as a result of lack of long-range order in amorphous graphitic materials [15]. It is possible to reproduce the experimental data with the help of a computer code by assuming two Gaussian curves to fit the two broad bands. The position (ω_i), width (Γ_i) and intensity (I_i) of each band were obtained by a least-squares best-fit procedure. The parameter values of this fitting procedure are quoted in Table 2. From this table, it is evident that the D band position is almost independent of the annealing temperature. In contrast, its relative intensity with respect to the G band is strongly temperature dependent. Both the wavenumber and bandwidth of the G band, as well as the I_D/I_G intensity ratio, are sometimes used as graphitization indices with the aim of relating the features of the Raman spectrum to the nanometric scale structure of carbon films [14,16]. In this regard, the observed line narrowing, especially the narrowing of the G band, accompanied by the shift of the G band peak position to higher frequencies and the increase of the I_D/I_G as a function of the annealing temperature might reflect a progressive increase of the number and/or size of the graphitic domains [14].

Raman spectra obtained from germanium-richer samples (a-$Ge_{0.57}C_{0.43}$ and a-$Ge_{0.76}C_{0.24}$; see Table 1) show spectral features due to transverse acoustic (at about $90 \, cm^{-1}$) and transverse optic (in the region between 200 and $300 \, cm^{-1}$) Ge–Ge modes [17]. Ge–Ge optic modes merge up into a sharp band peaked at about $300 \, cm^{-1}$ after thermal treatment at 550 °C, thus indicating the formation of crystalline Ge. This spectral evolution is clearly evidenced in Fig. 2, where the micro-Raman spectra obtained in the region between 220 and $370 \, cm^{-1}$ from a-$Ge_{0.76}C_{0.24}$ films annealed at some temperatures are plotted. The Raman spectra from as-deposited and samples annealed at temperatures up to 500 °C show a broad band centered at about $275 \, cm^{-1}$, typical of amorphous germanium. Similar measurements carried out from the a-$Ge_{0.57}C_{0.43}$ films indicate that Ge crystallization also occurs for annealing
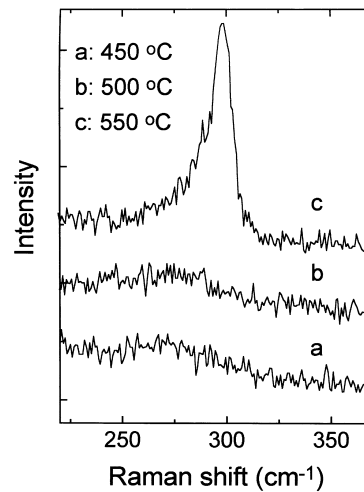

Fig. 2. Micro-Raman spectra obtained from annealed a-$Ge_{0.76}C_{0.24}$ films. Only the region of the optical modes of germanium is shown.

temperatures of 550 °C. For both film compositions, no Raman band associated with Ge–C modes was observed, neither in as-deposited nor in annealed samples, independent of the annealing temperature.

Fig. 3 reports the spectra observed in the region between 800 and $2000 \, cm^{-1}$ from as-deposited a-$Ge_{0.57}C_{0.43}$ film (Fig. 3a) and from the same sample after annealing at 550 °C (Fig. 3b). The occurrence of two weak bands, peaked at about $1370 \, cm^{-1}$ and $1580 \, cm^{-1}$, in the sample treated at 550 °C indicates that thermal annealing causes the formation of graphitic domains too. In contrast to what occurs in carbon films, visible light in Ge and in Ge-rich materials is strongly attenuated, and when the 488.0 nm laser line is used as excitation light, the sample depth probed by Raman scattering in pure Ge is shallower than 8 nm [18]. The
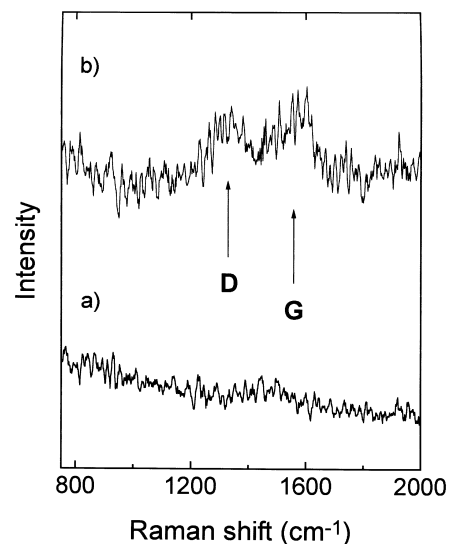
Table 2
Parameters of the Gaussian curves used to fit the D and G bands of Raman spectra obtained from annealed a-$Ge_{0.04}C_{0.96}$ films

Temperature (°C)	ω_D (cm^{-1})	Γ_D (cm^{-1})	ω_G (cm^{-1})	Γ_G (cm^{-1})	I_D/I_G
As-deposited	1363	298	1536	145	1.3
450	1380	291	1574	96	3.3
500	1377	283	1580	91	3.6
550	1368	278	1580	95	3.4

Fig. 3. Raman spectra obtained from: (a) as-deposited a-$Ge_{0.57}C_{0.43}$ film; and (b) the same sample after annealing at 550 °C.

extinction of exciting radiation can partially explain the poor statistics of Raman spectra obtained from our Ge-rich samples and, in particular, the absence of any Raman signal that could be attributed to any disordered or graphitic form of carbon in the spectra carried out from a-$Ge_{0.76}C_{0.24}$ films. In fact, Raman spectra of a-$Ge_{0.76}C_{0.24}$ samples annealed at 550 °C do not show any significant feature in the wavenumber region between 1250 and 1550 cm^{-1}.

A SEM image recorded from a representative region of the a-$Ge_{0.76}C_{0.24}$ film annealed at 550 °C is shown in Fig. 4a. The micrograph suggests the existence of an apparently uniform distribution of clusters at the sample surface. The micro-Raman spectrum reported in Fig. 4b has been carried out from such a region. Similar spectra were observed from different sample regions with the same morphology: Raman results definitively indicate that a uniform precipitation of Ge crystallites has occurred in a-$Ge_{0.76}C_{0.24}$ films annealed at 550 °C. In fact, all Raman spectra consist of a broad asymmetric band, peaked at lower energy with respect to the Raman peak of c-Ge. These spectral features are a typical manifestation of the confinement of optical phonons in quantum structures, a well recognized effect in microcrystalline semiconductor materials, in particular in μ-Si [19,20] and μ-Ge [21,22]. Both frequency shift and asymmetric broadening of the first-order Raman scattering are usually associated with finite size effects or with the average separation between defects and/or impurities in microcrystals, which destroy the full translational

symmetry of the system [19]. Using the approach suggested by dos Santos and Torriani [22] to reproduce the observed spectral intensity, the spectrum of Fig. 4b can be satisfactorily reproduced (continuous line), assuming a crystallite mean size $L = 4.3$ nm and a Gaussian distribution with mean value L and standard deviation $\sigma = 0.9$ nm to account for the inhomogeneous distribution of crystal sizes. The quite small value of the σ parameter indicates a nearly homogeneous distribution of crystal sizes within the probed regions in films annealed at 550 °C.

4. Summary and conclusions

In summary, our results reveal that amorphous carbon–germanium films, a-$Ge_{1-x}C_x$, deposited by d.c. magnetron sputtering are stable under thermal annealing at temperatures up to 300 °C. In the case of carbon-rich films ($x > 0.43$), Raman measurements suggest a progressive graphitization of the films, with graphitic nanoclusters increasing in size and/or number with the annealing temperature. For the germanium-rich films, the Raman results indicate the formation of a nearly homogeneous distribution of Ge nanocrystals, dispersed in an amorphous carbon–germanium matrix. However, the features observed in SEM images suggest larger grain sizes. These discrepancies can be explained by the fact that each technique is probing a different correlation length; Raman results probably reflect the average sepa-
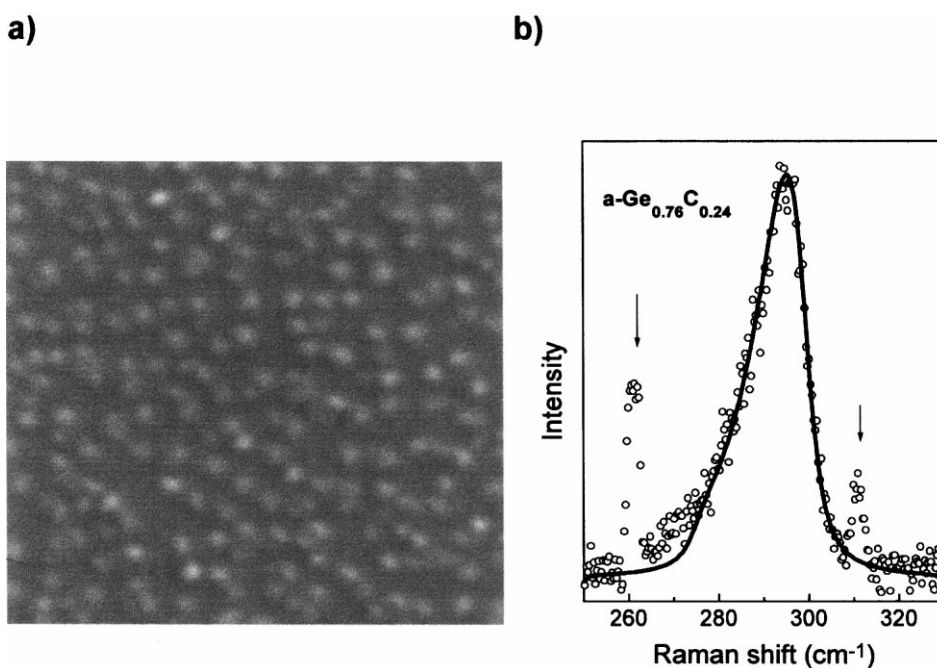
a)

b)

Fig. 4. (a) SEM image obtained from the a-$Ge_{0.76}C_{0.24}$ film annealed at 550 °C (40 000 ×). (b) Micro-Raman spectrum obtained from the same sample (dots). The continuous line represents the best fit obtained using the phonon confinement model [22]. Details of the procedure as well as the parameter values are reported in the text. The arrows indicate the position of the plasma lines at 261.3 and 311.1 cm^{-1} that were used for the precise determination of the Ge peak position.

ration between defects and/or impurities in the microcrystals.

Acknowledgements

References

[1] R.W. Collins, C.C. Tsai, M. Hirose, F. Koch, L. Bruns (Eds.), Microcrystalline and Nanocrystalline Semiconductors, Materials Research Society, Pittsburgh, PA, 1995.

[2] X. Shao, S.L. Rommel, B.A. Orner, H. Feng, M.W. Dashiell, R.T. Troeger, J. Kolodzey, P.R. Berger, T. Lauren, Appl. Phys. Lett. 72 (1998) 1860.

[3] E.S. Kim, N. Usami, Y. Shiraki, Appl. Phys. Lett. 72 (1998) 1617.

[4] C.K. Seal, D. Samara, S.K. Banerjee, Appl. Phys. Lett. 71 (1997) 3564.

[5] O.G. Schmidt, C. Lange, K. Eberl, O. Kienzle, F. Ernst, Appl. Phys. Lett. 71 (1997) 2340.

[6] M. Meléndez-Lira, J. Menéndez, W. Windl, O.F. Sankey, G.S. Spencer, S. Sego, R.B. Culbertson, A.E. Blair, T.L. Alford, Phys. Rev. B 54 (1996) 12866.

[7] B.-K. Yang, M. Krishnamurthy, W.H. Weber, J. Appl. Phys. 82 (1997) 3287.

[8] X.L. Wu, T. Gao, X.M. Bao, F. Yan, S. Jiang, D. Feng, J. Appl. Phys. 82 (1997) 2704.

[9] T. Kobayashi, T. Endoh, H. Fukuda, S. Nomura, A. Sakai, Y. Ueda, Appl. Phys. Lett. 71 (1997) 1195.

[10] R. Carles, A. Mlayah, M. Amjoud, A. Reynes, R. Morancho, Jpn. J. Appl. Phys. 31 (1992) 3511.

[11] T.-M. John, P. Veit, R. Anton, T. Drüsedau, Thin Solid Films 296 (1997) 69.

[12] J. Vilcarromero, F.C. Marques, F.L. Freire Jr., J. Appl. Phys. 81 (1998) 174.

[13] L.G. Jacobsohn, F.L. Freire Jr., G. Mariotto, Diamond Relat. Mater. 7 (1998) 440.

[14] R.O. Dillon, J.A. Woollam, V. Katkanant, Phys. Rev. B 29 (1984) 3482.

[15] F. Tuinstra, J.L. Koening, J. Chem. Phys. 53 (1970) 1126.

[16] G. Mariotto, F.L. Freire Jr., C.A. Achete, Thin Solid Films 241 (1994) 225.

[17] J.S. Lannin, in: Semiconductor and Semimetals, vol. 21, Academic Press, New York, 1984, chapter 6.

[18] J.M. Zhang, M. Giehler, A. Göbel, T. Ruf, M. Cardona, E.E. Haller, K. Itoh, Phys. Rev. B 57 (1998) 1348.

[19] H. Richter, Z.P. Zhang, W. Ley, Solid State Commun. 39 (1981) 625.

[20] I.H. Campbell, P.M. Fauchet, Solid State Commun. 58 (1986) 739.

[21] N.N. Ovsyuk, E.B. Gorokhov, V.V. Grishenko, A.P. Shebanin, JETP Lett. 47 (1988) 298.

[22] D.R. dos Santos, I.L. Torriani, Solid State Commun. 85 (1993) 307.